Cancer Immunology, Immunotherapy (2025) 74:237
https://doi.org/10.1007/s00262-025-04087-z

RESEARCH

Assessment of compartment-specific CD103-positive cells for prognosis prediction of colorectal cancer

Anpei Huang[1,2,3] · Yuanhui Wu[1,2,3] · Ji Cui[4] · Muyan Cai[5] · Yumo Xie[1,2,3] · Jialin Zou[6] · Maram Alenzi[7] · Hui Yang[8] · Pinzhu Huang[1,2,3,7] · Meijin Huang[1,2,3]

Received: 24 October 2024 / Accepted: 12 May 2025

Abstract

Background $CD103^+$ tissue-resident memory T cells was detected in various solid malignancies, like colorectal cancer (CRC), and associated with improved survival. However, clinical significance of $CD103^+$ cells in specific intratumor compartment remains unclear.

Methods The abundance and distribution of $CD103^+$ cells were assessed using immunohistochemistry and quantified separately for 3 compartments, including intraepithelial compartments at center of tumor (CT-IEL), stromal compartments at center of tumor (CT-ST) and invasive margin (IM) in a cohort of 224 CRC patients under radical surgery and correlated with outcome. Findings in each compartment were then validated in an external validation cohort comprising 294 CRC patients.

Results Elevated density of $CD103^+$ cells infiltration in the CT-IEL, CT-ST or IM compartment was correlated with favorable survival in both the initial discovery cohort and subsequent validation cohort. Notably, abundant $CD103^+$ cells located in the CT-IEL compartment was remained an independent prognostic indicator for CRC patients by multivariant analysis. Characterization study showed that intraepithelial $CD103^+$ cells were predominantly single positive CD8 T cells. Conversely, $CD103^+$ cells exhibited a heterogeneous population comprising $CD103^+CD8^+$ cells, $CD103^+CD4^+$ cells, and nonconventional $CD103^+CD4^+CD8^+$ cells in the CT-ST and IM compartments. Finally, a CD103 score was generated comprising abundance of $CD103^+$ cells in the 3 compartments. This score had the highest relative contribution to the risk of all clinical parameters for prognosis in both cohorts.

Conclusion This study supported a phenotypic heterogeneity of $CD103^+$ cells in CRC, and provided a reliable estimate of the risk of death and recurrence in CRC patients based on combined analysis of $CD103^+$ cells within 3 intratumor compartments.

Keywords Colorectal cancer · $CD103^+$ cell · Intratumor compartment · Prognosis

Abbreviations

CRC	Colorectal cancer
CSS	Cancer-specific survival

Anpei Huang, Yuanhui Wu and Ji Cui have contributed equally to this work and share first authorship.

✉ Pinzhu Huang
huangpzh3@mail.sysu.edu.cn

✉ Meijin Huang
hmjin@mail.sysu.edu.cn

[1] Department of Colorectal Surgery, The Sixth Affiliated Hospital, Sun Yat-Sen University, Guangzhou 510655, Guangdong, China

[2] Biomedical Innovation Center, The Sixth Affiliated Hospital, Sun Yat-Sen University, Guangzhou 510655, Guangdong, China

[3] Guangdong Provincial Key Laboratory of Colorectal and Pelvic Floor Diseases, The Sixth Affiliated Hospital, Sun Yat-Sen University, Guangzhou 510655, Guangdong, China

[4] Department of Gastrointestinal Surgery, The First Affiliated Hospital, Sun Yat-Sen University, Guangzhou 510080, Guangdong, China

[5] Department of Pathology, Cancer Center, Sun Yat-Sen University, Guangzhou 510050, Guangdong, China

[6] Department of Anorectal Surgery, Shenzhen Longgang Central Hospital, Shenzhen 518116, Guangdong, China

[7] Department of Medicine, Division of Gastroenterology, Hepatology and Nutrition, Beth Israel Deaconess Medical Center, Harvard Medical School, Boston, MA 02215, USA

[8] Department of Radiology, Cancer Center, Sun Yat-Sen University, Guangzhou 510050, Guangdong, China

Published online: 07 June 2025

CT-IEL	The intraepithelial compartments at center of tumor
CT-ST	The stromal compartments at center of tumor
DFS	Disease-free survival
IM	Invasive margin
mIF	Multiplex immunofluorescence
TRM	Tissue-resident memory T cells

Introduction

Colorectal cancer (CRC) is a prevalent gastrointestinal malignancy, ranking as the second leading cause of tumor-related deaths globally [1–3]. Currently, the primary method utilized by healthcare professionals to assess the prognosis of CRC patients is the AJCC/TNM staging system and tumor cell differentiation [2]. Nevertheless, due to the significant heterogeneity, patients with identical tumor stages may result in disparate responses to identical treatments, ultimately yielding variable clinical outcomes. This highlights the limitations of anatomy-based staging systems in predicting prognosis [4]. There is increasing recognition in literatures that the infiltration of immune cells in CRC has been shown to be superior to standard staging systems as a prognostic factor [5, 6]. Furthermore, the remarkable efficacy of immunotherapy in anti-tumor treatment has reignited interest in the role of tumor-infiltrating immune cells in cancer research [7, 8].

Tissue-resident memory T cells (TRM) represent a unique type of long-lived memory T cells capable of residing in tissues and participating in rapid immune responses against invading pathogens [9]. The infiltration of TRM cells within tumors has been linked to enhanced survival rates in various solid malignancies [10]. Recent investigations have identified CD103 as a canonical marker for TRM cells [10]. $CD8^+$ cells exposed to specific antigens within a TGF-β-enriched tumor microenvironment can upregulate CD103 expression and differentiate into $CD8^+$ TRM cells. The interplay between CD103 and E-cadherin significantly influences the recruitment and stimulation of $CD8^+$ TRM cells within tumor tissues, leading to the secretion of perforin and granzyme B and subsequently bolstering the anti-tumor immune response[11]. Studies have indicated that high infiltration of $CD103^+$ cells correlate with improved clinical outcomes in ovarian cancer, breast cancer, lung cancer, and CRC [12–15]. It has been recognized that a significant of $CD103^+$ cells in the tumor microenvironment concurrently express the CD8 molecule [10, 11, 16]. However, there are also different opinions that CD103 is also expressed at high levels on tumor-infiltrating regulatory T cells (Treg) and tumor-derived $CD103^+$ Treg suppress $CD8^+$ T cell responses more strongly than $CD103^-$ Treg [17–19]. Furthermore, It is also known that CD103 is the marker for dendritic cells and tumor-infiltrating $CD103^+$ dendritic cells are necessary for anti-tumor immunity [20]. Therefore, $CD103^+$ cells exhibit significant heterogeneity within the tumor microenvironment.

Tumor-infiltrating immune cells exhibit significant spatial heterogeneity within a single tumor section. Research has indicated that $CD8^+$ T cells located in the invasive margin (IM) are more numerous but also more functionally impaired compared to those found in the central of the tumor (CT) [21, 22]. Additionally, various immune cell populations such as $CD8^+$, $FOXP3^+$, and $CD45RO^+$ T cells demonstrate varying densities and prognostic implications in the intraepithelial compartment (CT-IEL) and stromal compartment of the central tumor (CT-ST) [23–25]. Similarly, $CD103^+$ cells in the CT-IEL compartment exhibited better survival than those in the CT-ST compartment of non-small cell lung cancer (NSCLC) [14]. Therefore, the anti-tumor efficacy of tumor-infiltrating immune cells is significantly influenced by their spatial localization and functional subpopulations. Previous study of $CD103^+$ cells in CRC have utilized immunohistochemical tissue microarray (TMA) technique [15]. The tumor tissue areas of TMA cores were liminted, which hinder the precise quantification of intratumoral $CD103^+$ cells in different compartments. Hence, a comprehensive characterization of $CD103^+$ cell phenotypes and their functional roles within specific intratumoral compartments may provide insights into the immune functions of $CD103^+$ cells in CRC.

Therefore, our study aimed to investigate the density, phenotype and prognostic value of $CD103^+$ cells within specific CRC intratumor compartments. Additionally, we developed an CD103 score based on the infiltration of $CD103^+$ cells in intratumor compartments to enhance the prognostic value of $CD103^+$ cells in CRC.

Materials and methods

Patient cohorts

This study encompassed two independent cohorts of CRC patients. The discovery cohort consisted of 224 patients who received treatment for CRC between January 2009 and December 2012 in the Colorectal Surgery Department at the Sixth Affiliated Hospital of Sun Yat-sen University (SYSUSH). The validation cohort included 294 CRC patients treated at the Cancer Center of Sun Yat-sen University (SYSUCC) between January 2004 and September 2005. All patients in both cohorts underwent curative resection, exhibited no distant metastasis, and did not receive preoperative anti-cancer therapy. Cancer staging was conducted in accordance with the 7th edition of the TNM classification system established by the American Joint Committee

on Cancer. Written informed consent was obtained from each patient, and the study was approved by the Clinical Research Ethics Committee of the Sixth Affiliated Hospital and the Cancer Center of Sun Yat-sen University. The primary objectives were to evaluate the prognostic significance of $CD103^+$ cell density in relation to cancer-specific survival (CSS) and disease-free survival (DFS). CSS was defined as the duration from tumor resection to death attributable to cancer. DFS was defined as the period from the date of surgery to first observation of disease recurrent.

Immunohistochemistry

The CRC samples were sectioned into 4 μm slices and used for immunohistochemical staining. The tissue sections underwent deparaffinization in xylene followed by rehydration through a graded series of alcohol solutions. Antigen retrieval was performed via microwave treatment in Tris–HCl buffer (pH 9.2). To inhibit endogenous peroxidase activity, the sections were treated with a 0.3% hydrogen peroxide (H_2O_2) solution. The sections were then blocked with goat serum at room temperature for 30 min and incubated with a monoclonal anti-CD103 primary antibody (Abcam) overnight at 4 °C. Subsequently, the sections were incubated with horseradish peroxidase-conjugated secondary antibodies (DAKO) at 37 °C for 30 min. Detection was performed using diaminobenzidine, followed by counterstaining with hematoxylin. Finally, the sections underwent washing, dehydration, and fixation.

Immunohistology evaluation

The density of $CD103^+$ cells within CT-IEL, CT-ST, and IM was analyzed by two independent observers who were blinded to patient outcomes and other clinical findings. The areas of CRC tissue were initially screened at low power (100 × magnification), and the five most representative high-power fields were subsequently captured at 400 × magnification for distinct tumor compartments in each specimen. The total number of $CD103^+$ infiltrating cells in each field was counted manually, and the mean value across five fields was calculated to determine the score for each tumor compartment. Finally, the average of the scores from the two independent observers was computed and employed as the definitive value for statistical analysis. To mitigate the impact of inter-cohort variation, we determined independent, cohort-specific thresholds based on the density of $CD103^+$ cells for each cohort. The cutoff value was defined as the lower tertile of $CD103^+$ cell density. In the discovery cohort, the cutoff values for $CD103^+$ cells in the CT-IEL, CT-ST, and IM compartments were 17.40, 26.90, and 38.30 per field, respectively. In the validation cohort, the corresponding cutoff values were 14.10, 20.00, and 26.80 per field, respectively.

Multiplex immunofluorescence staining

For multiplex immunofluorescence (mIF), the preparation and antigen retrieval of slides were conducted following standard immunohistochemistry protocols. The tyramide signal amplification (TSA) 4-Color IHC kit (abs50012-20T; Absin) was employed for mIF staining. Each slide underwent multiple rounds of staining, beginning with an overnight incubation of the primary antibody at 4℃. This was followed by a 30-min incubation with the corresponding secondary antibodies at 37℃, and subsequent covalent binding of TSA fluorophores. Specifically, anti-CD103 (Abcam), anti-CD4 (Abcam), and anti-CD8 (CST) antibodies were conjugated with TSA dye 520, TSA dye 570, and TSA dye 650, respectively. Nuclei were counterstained with DAPI.

Multiplex immunofluorescence imaging acquisition and analysis

The mIF slides were imaged and analyzed utilizing the TissueGnostics system. The composite multispectral images were decomposed into individual spectral images. Subsequently, appropriate positive thresholds for each biomarker were determined according to signal intensity, followed by the elimination of non-specific fluorescence. The correct nuclear signals were screened and then cell colocalization was performed to identify positive cells based on the membrane signal intensity of each biomarker. On this basis, the three most representative fields of each microcompartments were analyzed and counted all immune cell infiltrations per field.

CD103 score

Accorrding to the density of $CD103^+$ cells within each intratumoral compartment, patients were stratified into Int + Hi and Lo groups in both the discovery and validation cohorts. Subsequently, data from the CT-IEL, CT-ST, and IM compartments were consolidated and converted into a CD103 scoring system. Patients exhibiting Int + Hi density in all three compartments were classified as CD103 score of Hi. Those with Int + Hi density in any one or two of the compartments were classified as CD103 score of Int. Patients with low $CD103^+$ cell infiltration across all three compartments were classified as CD103 score of Lo.

Statistical analysis

The Kaplan–Meier method and log-rank test were utilized to evaluate survival outcomes between two distinct patient subgroups. Additionally, Cox proportional hazards models were employed to examine the impact of various covariates on survival, including $CD103^+$ cell density in different compartments, age, gender, histological type, histological grade, tumor location, T status, N status, vessel invasion, and perineural invasion. Hazard ratios (HR) and 95% confidence intervals (CI) for multivariate analyses were calculated using Cox proportional hazards regression models. Spearman correlation tests were used to analyze the associations of clinicopathological variables between the discovery and validation cohorts. The relationships between $CD103^+$ cell density and clinicopathological variables were assessed using the t-test. Multiple correlations of $CD103^+$ cell density across three intratumoral compartments were analyzed utilizing the multiple R-squared test. Chi-squared proportion tests were conducted to evaluate the relative contribution of each parameter to survival risk in CSS and DFS. All statistical tests were two-sided, with a significance threshold set at $P < 0.05$. The statistical analyses were performed using GraphPad Prism (version 8.02) and IBM SPSS Statistics (version 22) software.

Results

Patient characteristics

This study enrolled a total of 663 patients diagnosed with AJCC/UICC TNM stage I-III CRC, comprising 307 patients from SYSUSH and 356 patients from SYSUCC. A total of 145 patients were excluded from the analysis due to the absence of tumor paraffin wax in 65 patients and the lack of representative CT-ST or IM compartments in 80 patients. Consequently, 224 patients from SYSUSH were enrolled into the discovery cohort, while 294 patients from SYSUCC were assigned to the validation cohort (Fig. 1a). The demographic and clinical characteristics of the patients were well balanced between the discovery and validation cohorts, with the exception of the number of cases of mucinous adenocarcinoma (Table S1). Overall, patients were 55.8% male, and the median age was 60 years ([IQR] 51–69). Among the whole cohort, 101 patients (19.5%) were diagnosed with stage I CRC, 217 patients (41.9%) with stage II CRC, and 200 patients (38.6%) with stage III CRC. Across all patients, 119 (23.0%) experienced relapses, and 98 (18.9%) succumbed to CRC-related causes. The median follow-up time was 101.8 months for the discovery cohort and 106.5 months for the validation cohort. The median survival time from surgery to CRC-related death was 38.6 months.

The density of $CD103^+$ cells in different intratumoral compartments

To elucidate the density of $CD103^+$ cells, the tumor specimen of each patient was classified into three distinct regions: the intraepithelial compartments at the center of the tumor (CT-IEL), the stromal compartments at the center of the tumor (CT-ST), and the invasive margin (IM) (Fig. 1b). In the discovery cohort, the density of $CD103^+$ cells was found to be highest in the IM compartment, whereas the CT-IEL compartment exhibited the lowest density of $CD103^+$ cells among the three intratumoral compartments (Fig. 2a). Similar results were observed in both the validation cohort and the whole cohort; however, no significant difference was found in the density of $CD103^+$ cells between CT-IEL and CT-ST within the validation cohort (Fig. 2b, c). Additionally, the density of $CD103^+$ cells across the three intratumoral compartments demonstrated a strong correlation within the various patient cohorts (Fig. 2a, b, c).

Associations between the density of $CD103^+$ cells and clinicopathologic characteristics are listed in Table S2and Table S3. In the discovery cohort, tumors with a higher N stage or positive perineural invasion exhibited lower density of $CD103^+$ cells across all three intratumoral compartments. The density of $CD103^+$ cells in the CT-IEL and IM compartments were significantly reduced in patients who experienced postoperative recurrence and metastasis, a pattern not observed in the CT-ST compartment. In the CT-ST compartment, patients with a lower T stage demonstrated higher infiltration of $CD103^+$ cells. Mucinous adenocarcinoma exhibited lower infiltration of $CD103^+$ cells in the IM compartment. Unexpectedly, patient gender was correlated with the density of $CD103^+$ cells in CT-IEL compartment. In the validation cohort, patients presenting with higher T stage, higher N stage, or postoperative recurrence and metastasis demonstrated lower density of $CD103^+$ cells across all three intratumoral compartments. Mucinous adenocarcinoma showed diminished infiltration of $CD103^+$ cells in both the CT-ST and IM compartments. Additionally, poorly differentiated tumors were associated with lower infiltration of $CD103^+$ cells in the CT-ST compartment. No significant associations were observed between the density of $CD103^+$ cells with age or gender of patients in validation cohort.

Prognostic value of clinicopathologic characteristics in patient cohorts

Among the clinicopathologic characteristics of the discovery cohort, a higher N stage and positive vascular invasion were strongly associated with worse CSS (Fig. 2d). In terms of DFS,

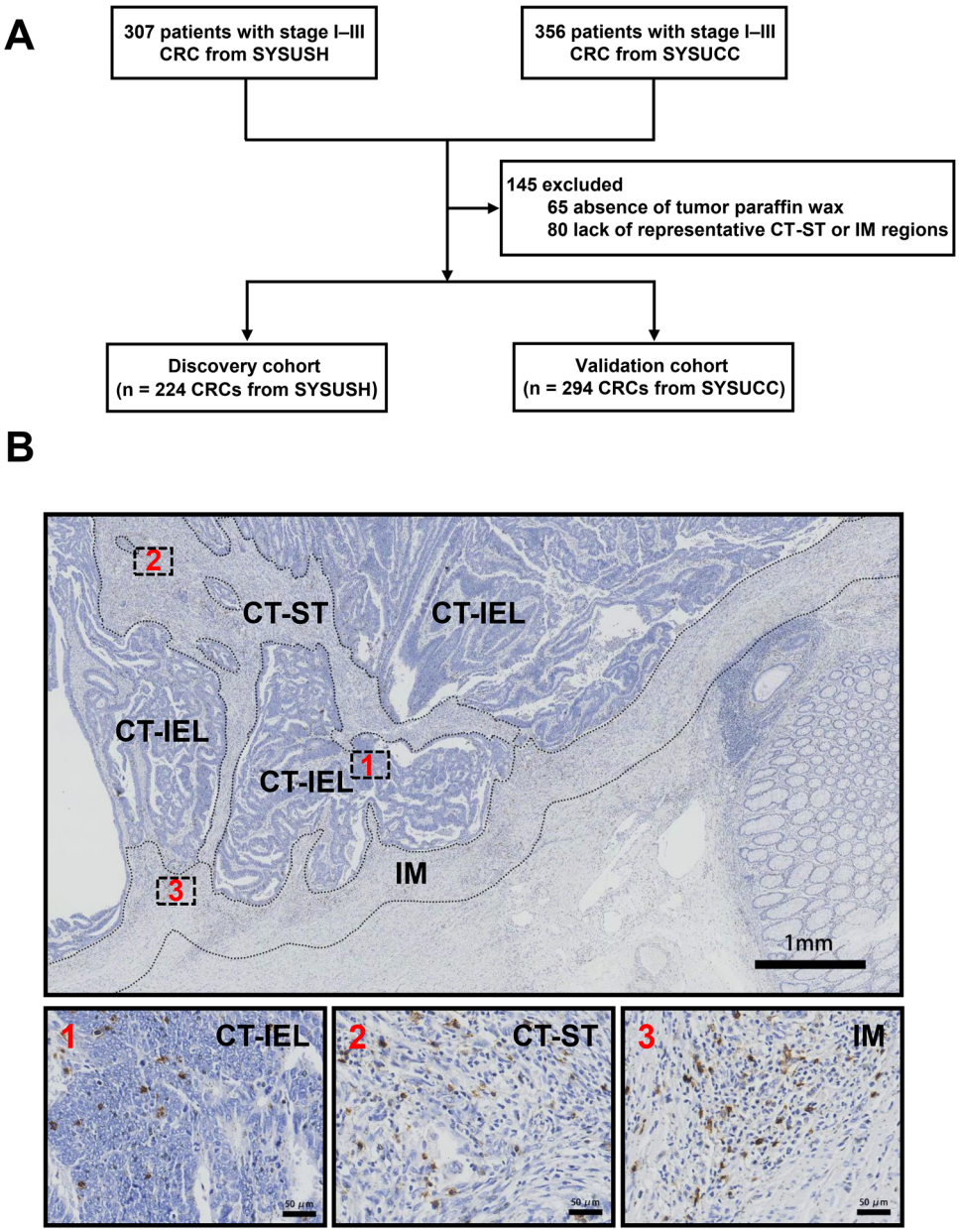

Fig. 1 Study design and representative images of CD103$^+$ cell infiltration in CRC tissues. **a** Study flowchart. **b** The upper part of the image illustrated the representative divisions of the CT-IEL, CT-ST, and IM compartments within CRC tissues. The lower part of the images presented representative examples of each intratumoral compartment utilized for immunohistological evaluation

female CRC patients exhibited a survival advantage compared to males, while a higher N stage remained a significant risk factor (Fig. 2e). In the validation cohort, patients with higher T and N stages presented significantly worse outcomes for CSS (Fig. 2d). In terms of DFS, patients with right-sided colon cancer had better outcomes and a higher N stage predict a worse risk for DFS (Fig. 2e). Across the whole cohort, tumor location and N stage were strongly associated with survival outcomes (Fig. 2d, e).

Prognostic value of CD103$^+$ cells within different intratumoral compartments on the survival of patients with CRC.

Based on the density of CD103$^+$ cells in each compartment, patients were stratified into three groups: high infiltration (Hi), intermediate infiltration (Int), and low infiltration (Lo), from highest to lowest (Table S4). The three-category Kaplan–Meier analysis identified patients with distinct

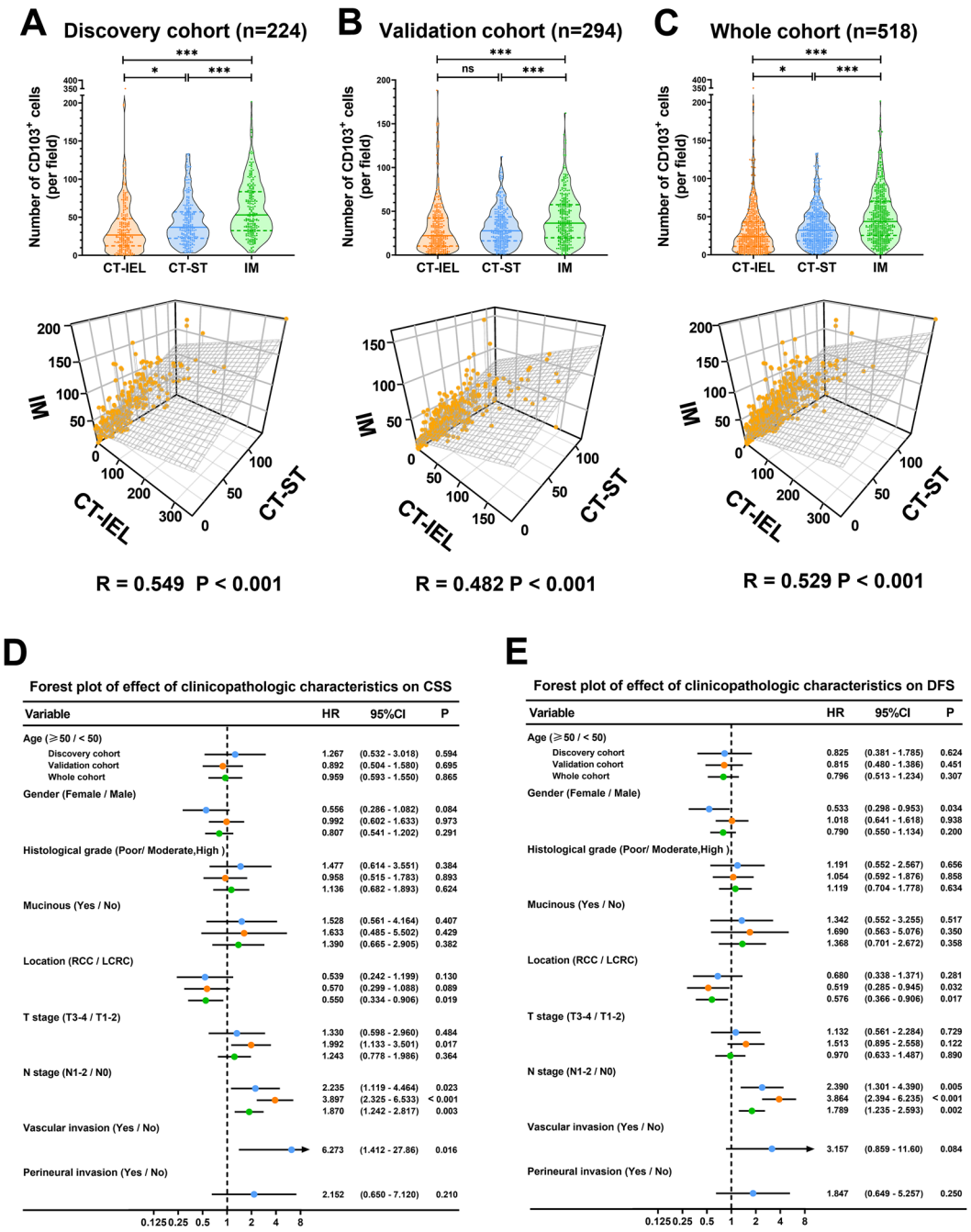

Fig. 2 The densities of CD103$^+$ cells in different compartments and prognostic value of clinicopathologic characteristics in patient cohorts. **a**, **b**, **c** The violin plots illustrated the densities of CD103$^+$ cells across distinct compartments for each patient cohort. **a**, **b**, **c** The scatter plots depicted the multivariate correlation of CD103$^+$ cells among three intratumoral compartments across various patient cohorts. **d**, **e** The forest plots represented the prognostic significance of clinicopathologic characteristics on CSS and DFS within each patient cohort. *$p < 0.05$, **$p < 0.01$, ***$p < 0.001$

clinical outcomes for CSS and DFS. However, no significant differences were observed between the Hi and Int groups across most subgroups (data not shown). Consequently, the Int and Hi groups were combined into a new group, designated as the Int + Hi group. The lower tertile of CD103$^+$ cell density was used as the cutoff value for each compartment. In the CT-IEL compartment, patients with high and intermediate levels of CD103$^+$ cell infiltration presented significantly better outcomes for CSS (Fig. 3a, p = 0.0005) and DFS (Fig. 3d, p = 0.0016) compared to patients with low levels of CD103$^+$ cell infiltration. Similarly, in the CT-ST compartment, patients in the Int + Hi group had a survival

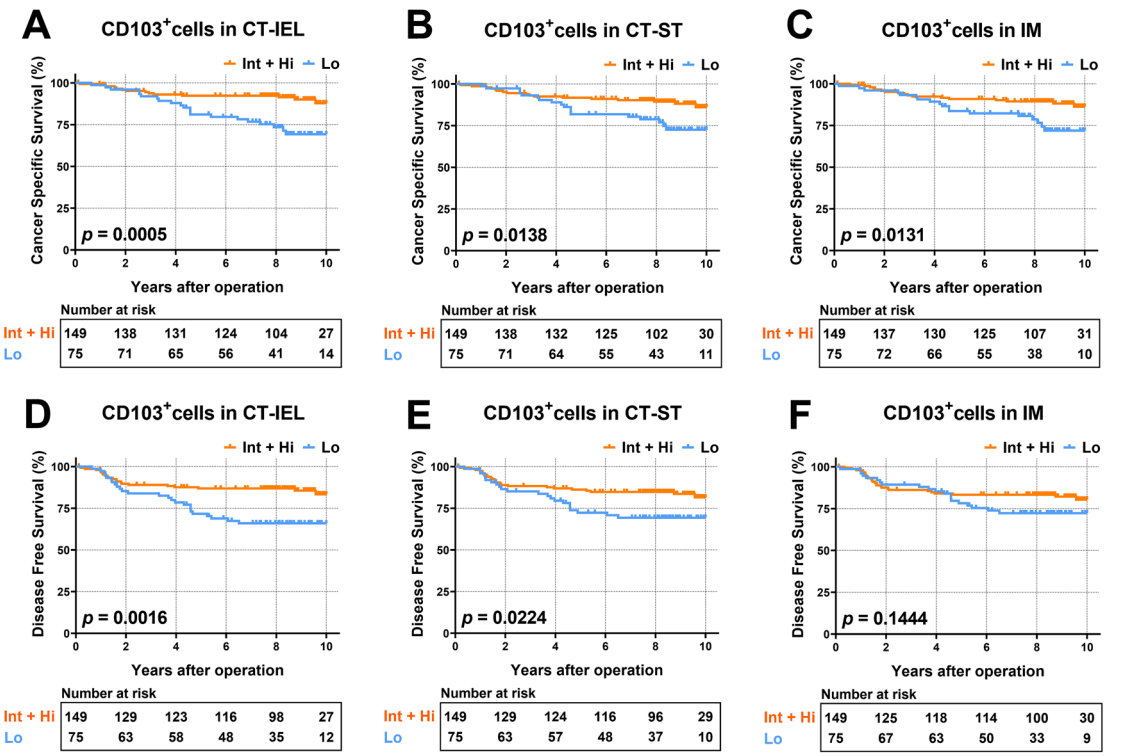

G

Multivariate analysis of prognostic factors for CSS and DFS in discovery cohort				
	Univariate		Multivariate	
Variable	P value	HR	95%CI	P value
CSS				
N stage (N1-2/ N0)	0.023	1.457	0.728 - 2.918	0.288
Vascular invasion (Yes / No)	0.016	2.976	1.129 - 7.843	0.027
CD103⁺ cells in CT-IEL (Lo/ Int+Hi)	< 0.001	2.309	1.007 - 5.298	0.048
CD103⁺ cells in CT-ST (Lo/ Int+Hi)	0.014	1.233	0.536 - 2.837	0.623
CD103⁺ cells in IM (Lo/ Int+Hi)	0.013	1.298	0.595 - 2.832	0.513
DFS				
Gender (Female/Male)	0.034	0.551	0.292 - 1.041	0.067
N stage (N1-2/ N0)	0.005	1.789	0.970 - 3.300	0.063
CD103⁺ cells in CT-IEL (Lo/ Int+Hi)	0.002	1.758	0.863 - 3.580	0.120
CD103⁺ cells in CT-ST (Lo/ Int+Hi)	0.022	1.249	0.621 - 2.513	0.532

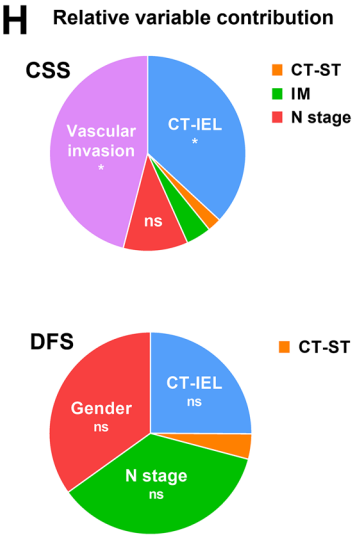

Fig. 3 The impact of different compartments of CD103$^+$ cell density on the outcomes of CRC patients in discovery cohort. Kaplan–Meier curves illustrated a beneficial effect of CD103$^+$ cell density in the CT-IEL (**a**, **d**) and CT-ST (**b**, **e**) compartments on CSS and DFS. In the IM compartment, CD103$^+$ cell density exhibited a positive effect on CSS, but not on DFS (**c**, **f**). **g** A Cox multivariable regression analysis of CSS and DFS was conducted, incorporating CD103$^+$ cells in the CT-IEL, CT-ST, and IM compartments alongside clinical parameters such as gender, N stage, and vascular invasion. **h** The relative contribution of each parameter to survival risk for CSS and DFS was assessed using a chi-squared proportion test. *$p<0.05$, **$p<0.01$, ***$p<0.001$

advantage in both CSS (Fig. 3b, p = 0.0138) and DFS (Fig. 3e, p = 0.0224) compared to those in the Lo group. In the IM compartment, high and intermediate CD103$^+$ cell infiltration was positively associated with CSS (Fig. 3c, p = 0.0131), while no significant effect was observed on DFS (Fig. 3f, p = 0.1444). Within the discovery cohort, a multivariate model was utilized to identify independent prognostic factors. This model encompassed all clinicopathological variables, along with various compartments of CD103$^+$ cell density, which exhibited significant prognostic value in the

univariate analysis. The results indicated that CD103$^+$ cell infiltration in the CT-IEL compartment and vascular invasion independently held prognostic significance for CSS (Fig. 3g). Subsequently, we analysed the relative contribution of each parameter to predict CSS and found that the most important variables were vascular invasion (46.0%) and CD103$^+$ cells in the CT-IEL compartment (36.9%, Fig. 3h). However, no variable exhibited independent prognostic significance for DFS (Fig. 3g).

To validate the findings derived from the discovery cohort, we incorporated a validation cohort comprising 294 CRC patients. Analogous to the discovery cohort, patients

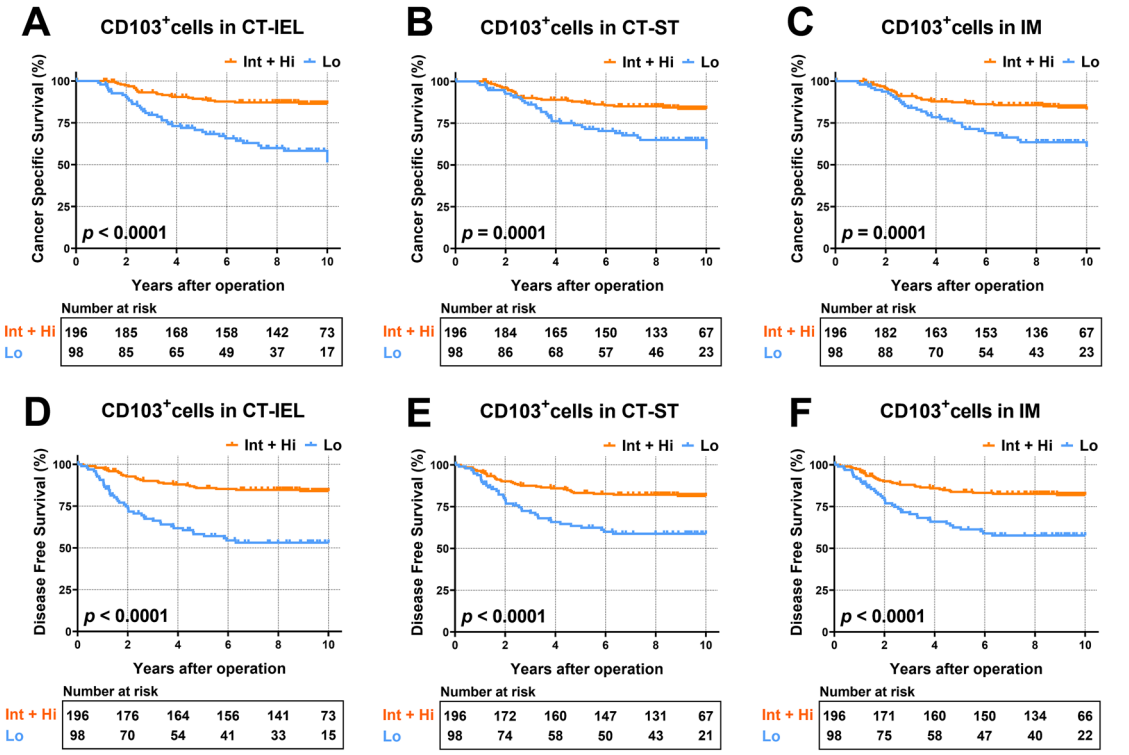

G

Multivariate analysis of prognostic factors for CSS and DFS in validation cohort				
	Univariate	Multivariate		
Variable	P value	HR	95%CI	P value
CSS				
T stage (T3-4/ T1-2)	0.017	1.460	0.678 - 3.146	0.334
N stage (N1-2/ N0)	< 0.001	2.711	1.551 - 4.739	< 0.001
CD103$^+$ cells in CT-IEL (Lo/ Int+Hi)	< 0.001	2.844	1.398 - 5.788	0.004
CD103$^+$ cells in CT-ST (Lo/ Int+Hi)	< 0.001	0.891	0.464 - 1.710	0.728
CD103$^+$ cells in IM (Lo/ Int+Hi)	< 0.001	1.244	0.666 - 2.321	0.493
DFS				
Location (RCC / LCRC)	0.032	0.404	0.175 - 0.934	0.034
N stage (N1-2/ N0)	< 0.001	2.774	1.672 - 4.604	< 0.001
CD103$^+$ cells in CT-IEL (Lo/ Int+Hi)	< 0.001	2.434	1.280 - 4.627	0.007
CD103$^+$ cells in CT-ST (Lo/ Int+Hi)	< 0.001	0.956	0.537 - 1.703	0.879
CD103$^+$ cells in IM (Lo/ Int+Hi)	< 0.001	1.487	0.840 - 2.632	0.173

H Relative variable contribution

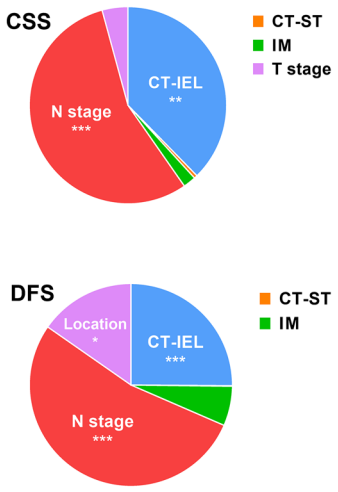

Fig. 4 Prognostic value of CD103$^+$ cell density in a validation cohort of CRC patients. The Kaplan–Meier survival analysis showed the probability of CSS and DFS, stratified according to the density of CD103$^+$ cells within the compartments of CT-IEL (**a**, **d**), CT-ST (**b**, **e**), and IM (**c**, **f**). **g** Cox multivariable regression analysis of CSS and DFS included CD103$^+$ cells in the CT-IEL, CT-ST, and IM compartments, along with clinical parameters such as T stage, N stage and location. **h** The relative contribution of each parameter to survival risk for CSS and DFS was assessed using a chi-squared proportion test. *$p < 0.05$, **$p < 0.01$, ***$p < 0.001$

in the validation cohort were categorized into Int + Hi and Lo groups based on the density of $CD103^+$ cells. Patients exhibiting high and intermediate infiltration of $CD103^+$ cells within the CT-IEL compartment demonstrated significantly prolonged survival for both CSS (Fig. 4a, $p < 0.0001$) and DFS (Fig. 4d, $p < 0.0001$). In the CT-ST compartment, the Int + Hi group significantly predicted a lower risk for CSS (Fig. 4b, $p = 0.0001$) and DFS (Fig. 4e, $p < 0.0001$) compared to the Lo group. Comparable outcomes were observed in the IM compartment, where the Int + Hi group demonstrated a positive impact on CSS (Fig. 4c, $p = 0.0001$) and DFS (Fig. 4f, $p < 0.0001$). In the multivariate analysis, the infiltration of $CD103^+$ cells in the CT-IEL compartment remained significant for CSS and DFS within a multivariable Cox model that included tumor location, T stage, N stage, and $CD103^+$ cell infiltration in three compartments (Fig. 4g). The variables with the most important relative contribution to the risk were as follows: for CSS, N stage (55.5%) and $CD103^+$ cells in CT-IEL (37.7%); for DFS, N stage (53.2%), $CD103^+$ cells in CT-IEL (25.1%), and location (15.3%) (Fig. 4h). Furthermore, we also analyzed the prognostic value of $CD103^+$ cells in the whole cohort and found that the most important variables were $CD103^+$ cells in CT-IEL (53.3%), N stage (25.1%), and location (16.1%) in CSS, and $CD103^+$ cells in CT-IEL (52.3%), N stage (25.7%), and location in DFS (17.2%, Figure S2).

Immunolocalization of different $CD103^+$ cell subpopulations in the intratumoral compartments of CRC tissues

$CD103^+$ cells, similar to many other tumor-infiltrating immune cells, exhibit significant heterogeneity within tumor tissues, with only certain subsets demonstrating antitumor activity. One study has indicated that the infiltration of $CD103^+CD4^+$ T cells is associated with lower survival rates in gastric cancer [26]. To identify the subset of $CD103^+$ cells across intratumoral compartments, we performed colocalization studies and calculated the frequency of $CD103^+$ cells co-expressing the T helper cells marker CD4 and the cytotoxic T cells marker CD8. The mIF staining revealed a substantial infiltration of both $CD103^+$ cells and $CD8^+$ T cells in the CT-IEL compartment, with approximately 72.2% of $CD103^+$ cells being $CD8^+CD103^+$ double-positive (DP) cells. In contrast, $CD4^+$ T cells in the CT-IEL compartment were scarce, with only 10.2% of $CD103^+$ cells co-stained with CD4 (Fig. 5a). Within the CT-ST compartment, approximately half (57.4%) of the $CD103^+$ cells were $CD8^+CD103^+$ DP cells. The frequencies of $CD4^+CD103^+$ DP cells were 14.9%. In addition, we identified a small population of $CD4^+CD8^+CD103^+$ triple-positive (TP) cells, constituting less than 5% of the total $CD103^+$ cell population (Fig. 5b). In the IM compartment, the proportion of colocalized cells among the total $CD103^+$ cells was comparable to that observed in the CT-ST compartment (Fig. 5c). Notably, the infiltration of $CD8^+CD103^+$ DP cells was higher in the CT-IEL compartment compared to the CT-ST and IM compartments (Fig. 5d). Conversely, the proportions of $CD4^+CD103^+$ DP cells and TP cells were lower in the CT-IEL compartment compared to the CT-ST and IM compartments (Fig. 4e, f). Collectively, these findings indicate that the CT-IEL compartment is predominantly characterized by a $CD8^+CD103^+$ DP lymphocyte phenotype among $CD103^+$ cells, whereas the CT-ST and IM compartments exhibit a more complex subpopulations of $CD103^+$ cells.

Combined assessment of $CD103^+$ cells density in different intratumoral compartments to predict clinical outcome

To differentiate patient subgroups with distinct clinical outcomes, CRC patients were categorized based on a CD103 score for $CD103^+$ cells within each intratumoral compartment (CT-IEL, CT-ST, IM). Patients were stratified into Int + Hi and Lo groups within each compartment according to the classifications established in the original cohort. Subsequently, data from CT-IEL, CT-ST, and IM were consolidated and transformed into a composite CD103 score. Using this composite CD103 score, three distinct CRC patient subgroups were identified (Lo, Int, and Hi). Patients exhibiting low infiltration of $CD103^+$ cells across all three tumor compartments were designated as having a CD103 score of Lo. Conversely, patients with intermediate to high density in all three compartments were assigned a CD103 score of Hi. Those with Int + Hi density in one or two of the three compartments were categorized with a CD103 score of Int. Based on this classification, 18.15, 31.47, and 50.39% of the whole cohort of CRC patients were classified into the Lo, Int, and Hi groups, respectively (Fig. 6a). Notably, patients with a CD103 score of Hi demonstrated the highest 5-year CSS rate at 92.0% and DFS rate at 88.5%. The Lo and Int groups presented with CSS and DFS rates at 5 years of 83.1 and 73.7, and 71.4 and 60.7%, respectively. Patients with a low CD103 score had shorter survival times. Kaplan–Meier analysis identified that patients in Lo group illustrated the significantly shorter CSS (Fig. 6b) and DFS (Fig. 6c) compared to those in the Int and Hi groups. Furthermore, patients with a high CD103 score exhibited significantly longer survival for both CSS and DFS compared to patients in the Int group. Utilizing Cox multivariate regression analysis, it was determined that the CD103 score, N stage, and tumor location were significantly and independently associated with CSS and DFS (Fig. 6d). The power of CD103 score to predict CSS and DFS was superior to that of the N stage and tumor location (Fig. 6e). These findings were consistent across both the discovery and validation cohorts,

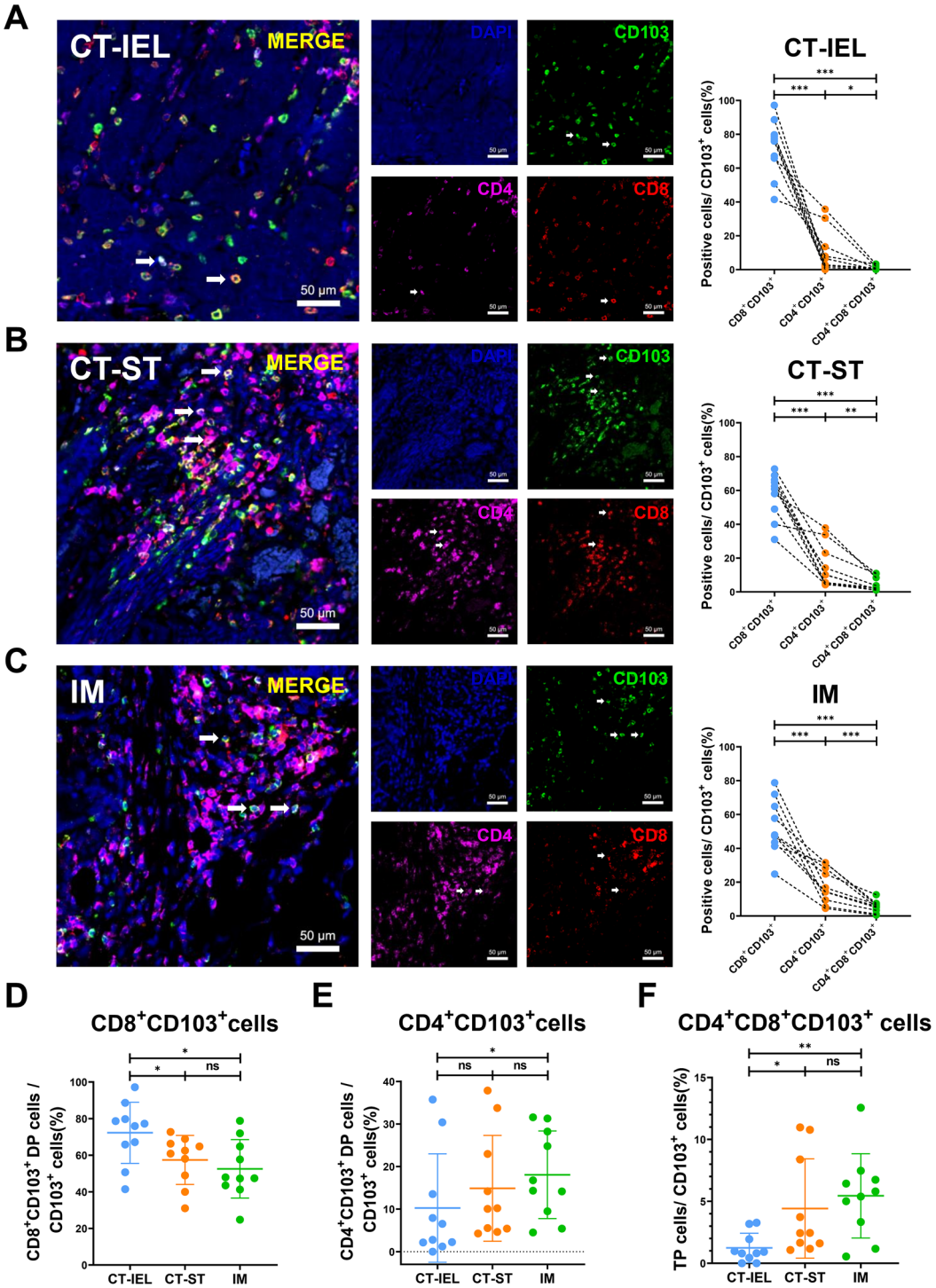

Fig. 5 Immunolocalization of different CD103$^+$ cell subpopulations in the intratumoral compartments of CRC tissues. The representative mIF staining illustrated the infiltration of CD103 (green), the T helper cell marker CD4 (violet), and the cytotoxic T cell marker CD8 (red) within the CT-IEL (**a**), CT-ST (**b**), and IM (**c**) compartments of CRC tissues. The proportion of cells positive for these markers relative to the total number of CD103$^+$cells is depicted for the CT-IEL (**a**), CT-ST (**b**), and IM (**c**) compartments of CRC tissues. (**d**) The proportion of CD8$^+$CD103$^+$ DP cells was observed to be higher in the CT-IEL compartment compared to the CT-ST and IM compartments. The proportions of CD4$^+$CD103$^+$ DP cells (**e**) and CD4$^+$CD8$^+$CD103$^+$ TP cells (**f**) were found to be lower in the CT-IEL compartment relative to the CT-ST and IM compartments. Scale bars indicate 50µm. *$p<0.05$, **$p<0.01$, ***$p<0.001$

establishing the CD103 score as an independent prognostic factor for patients with CRC. Furthermore, the relative contribution to the risk showed that CD103 score was better than all clinical variables (Figure S3, S4).

Prognostic value of CD103 score among patients with or without lymph node metastasis

In our research, lymph node metastasis is identified as an independent high-risk factor for patients in the validation cohort and the whole cohort. To assess the prognostic impact of CD103 score in patients without lymph node metastases (stage I-II CRC) and in those with lymph node metastases (stage III CRC), subgroup analyses were conducted based on N stage. The proportion of patients in the N stage subgroups was found to be similar to that of the overall group (Fig. 6f, i; overall v N = 0, $p = 0.7362$; overall v N = 1,2, $p = 0.5906$). In both N stage subgroups, a high CD103 score was correlated with longer survival among CRC patients. Lymph node negative patients with Hi CD103 score exhibited markedly superior survival outcomes for both CSS and DFS in comparison to those with Int and Lo CD103 scores (Fig. 6g, h). The intermediate group also displayed a greater impact on CSS and DFS than the Lo group. In patients with positive lymph node status, the high CD103 score group significantly associated with a lower risk for CSS and DFS compared to the Int and Lo CD103 score groups (Fig. 6j, k). However, there was no significant difference in CSS and DFS survival curves between the Int and Lo CD103 score groups. Therefore, CD103 score emerged as a significant predictor of survival in both stage I-II and stage III CRC patients.

Discussion

Our study included two independent cohorts from two hospitals, comprising a collective 518 patients with Stage I-III CRC. Elevated levels of $CD103^+$ cell infiltration in the CT-IEL, CT-ST, and IM compartments were found to be associated with improved survival outcomes in discovery and validation cohorts. $CD103^+$ cells located in CT-IEL compartment could serve as an independent prognostic factor for patients with CRC. Furthermore, the majority of $CD103^+$ cells within the CT-IEL compartment exhibited a $CD8^+CD103^+$ cell phenotype, whereas in the CT-ST and IM compartments, $CD103^+$ cells represented a heterogeneous population of cell phenotypes. Additionally, an CD103 score was formulated based on the infiltration of $CD103^+$ cells in intratumoral compartments, facilitating the delineation of patient subgroups with diverse clinical outcomes. These results imply that $CD103^+$ cells in various intratumor compartments, particularly the CT-IEL compartment, may serve as prognostic indicators for patients with CRC.

Previous research has demonstrated a significant correlation between $CD103^+$ cells and survival in NSCLC and ovarian cancer, without the need to discriminate their location in intraepithelial versus stromal compartments [12, 14]. Consistent with these findings, our study revealed that the infiltration of $CD103^+$ cells across all three intratumor compartments is associated with enhanced survival outcomes in two independent cohorts of CRC patients. The power of $CD103^+$ cells in the CT-IEL compartment for predicting survival was superior to that of $CD103^+$ cells in the CT-ST and IM compartments. Notably, only $CD103^+$ cells in the CT-IEL compartment function as an independent prognostic factor for patients with CRC. Similar with our findings, $CD103^+$ cells within the intraepithelial compartment also serve as an independent prognostic factor in NSCLC and urothelial cell carcinoma of the bladder (UCB) [14, 27]. The protective role of $CD103^+$ cells in the intraepithelial compartment of different tumors, along with their superior clinical survivals, may be attributed to their epithelium-favored infiltration pattern. E-cadherin, the natural ligand for CD103, facilitates the persistent residency and anti-tumor immune response of $CD103^+CD8^+$ cells [11]. Our study found a positive correlation between $CD103^+$ cells and E-cadherin expression within the intraepithelial compartment (Figure S5), which is consistent with previous studies in UCB and prostate cancer [27, 28].

The intratumoral distribution and prognostic value of $CD103^+$ cells are also influenced by their functional subpopulations. Previous studies have showed coexpression of CD103 and CD8 in CRC tissues [15]. In our study, we observed that the majority of $CD103^+$ cells within the CT-IEL compartment were $CD103^+CD8^+$ cells. Conversely, the CT-ST and IM compartments exhibited a heterogeneous population comprising $CD103^+CD8^+$ cells, $CD103^+CD4^+$ cells, and nonconventional $CD103^+CD4^+CD8^+$ cells. It is widely accepted that mature peripheral T cells express either CD4 or CD8, but not both. Within the tumor microenvironment, $CD8^+$ T cells predominantly engage in anti-tumor cytotoxic activities, while $CD4^+$ T cells perform helper functions to regulate the immune response. However, mature $CD4^+CD8^+$ T cells have been identified in various tumor tissues, and their origin and biological functions remain largely unknow [29]. A study on melanoma revealed that intratumoral $CD4^+CD8^+$ T cells originate from $CD8^+$ T cells and exhibit transitional characteristics from a cytotoxic effect to a helper function [30]. In renal cell carcinoma, $CD4^+CD8^+$ T cells represent a subpopulation of $CD8^+$ T cells characterized by the upregulation of CD4 expression. This observation led the authors to propose that these cells are the result of an antigen-driven expansion of $CD8^+$ T cells and subsequently differentiation into a $CD4^+CD8^+$ T cell phenotype [31]. Furthermore, it has been reported that metastatic CRC samples exhibit a higher proportion of $CD4^+CD8^+$ T

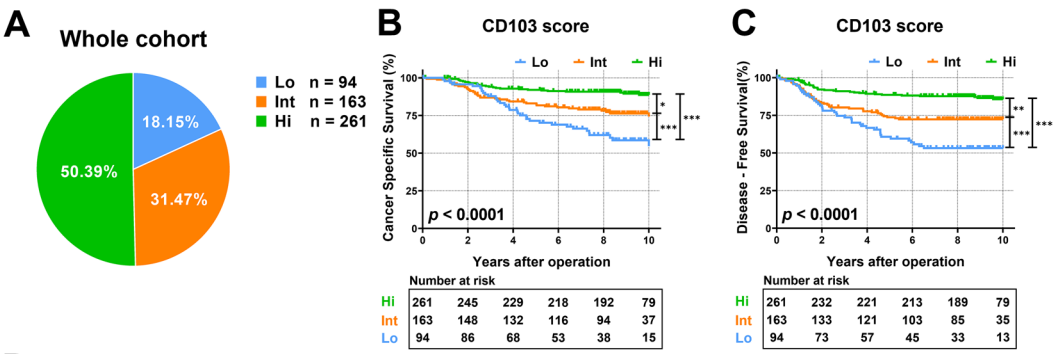

D

Multivariate analysis of prognostic factors for CSS and DFS in whole cohort

	Univariate		Multivariate	
Variable	P value	HR	95%CI	P value
CSS				
Location (RCC / LCRC)	0.019	0.497	0.258 - 0.957	0.037
N stage (N1-2/ N0)	0.003	1.703	1.143 - 2.536	0.009
CD103 score	< 0.001			< 0.001
Int vs Lo	0.010	0.581	0.365 - 0.925	0.022
Hi vs Lo	< 0.001	0.235	0.141 - 0.391	< 0.001
DFS				
Location (RCC / LCRC)	0.017	0.530	0.298 - 0.943	0.031
N stage (N1-2/ N0)	0.002	1.635	1.140 - 2.345	0.008
CD103 score	< 0.001			< 0.001
Int vs Lo	0.007	0.582	0.380 - 0.892	0.013
Hi vs Lo	< 0.001	0.259	0.164 - 0.408	< 0.001

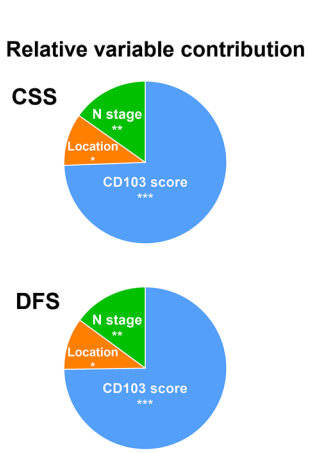

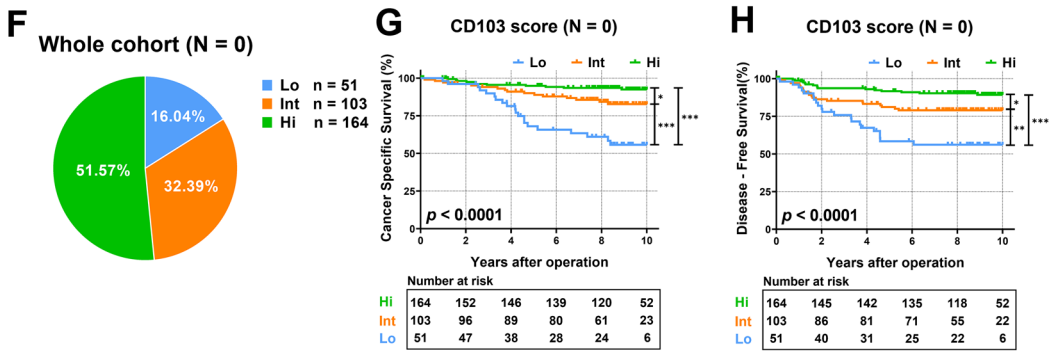

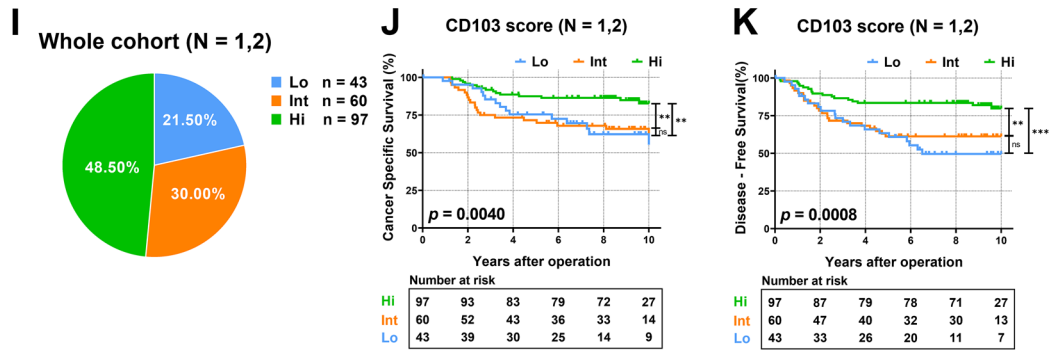

cells compared to non-metastatic CRC samples and normal colonic mucosa. These cells have been reported to promote tumor growth or metastasis and/or suppress immune responses in CRC through their high capacity to secrete IL-4 and IL-13 [32]. Another study identified that there are a population of T cells co-expresses both CD4 and CD8a in the human colonic mucosa and blood, which displays a type 1-like T regulatory cells phenotype and play a role in colon homeostasis [33]. In connection with the aforementioned literature, we hypothesize that these $CD103^{+}CD4^{+}CD8^{+}$ cells

◂**Fig. 6** The impact of CD103 score on the outcome of whole cohort of CRC patients. Kaplan–Meier survival analysis was conducted to assess CSS and DFS in 518 CRC patients, stratified by the densities of $CD103^+$ cells across various intratumoral compartments (CT-IEL, CT-ST, and IM). **a** The pie charts illustrated the proportion of the three CD103 score groups within whole cohort. **b**, **c** The Kaplan–Meier survival analysis showed the probability of CSS and DFS stratified by CD103 score. **d** Cox multivariable regression analysis of CSS and DFS included CD103 score, N stage and location. **e** The relative contribution of each parameter to survival risk for CSS and DFS was assessed using a chi-squared proportion test for CD103 score, N stage, and location. The pie charts illustrated the proportions of the three CD103 score groups among patients without (**f**) and with lymph node metastasis (**i**). The Kaplan–Meier curves represented the probability of CSS and DFS in relation to the CD103 score among patients without (**g**, **h**) and with lymph node metastasis (**j**, **k**). $*p<0.05$, $**p<0.01$, $***p<0.001$

may be more closely associated with immunosuppressive or immune regulatory functions rather than direct anti-tumor immune effects. The expression of CD103 indicates a tumor-resident phenotype of $CD4^+CD8^+$ T cells, suggesting that these cells are mature peripheral T cells rather than naïve $CD4^+CD8^+$ T cells. In addition, one study has shown that the infiltration of intratumoral $CD103^+CD4^+$ T cells is associated with decreased survival rates in gastric cancer [26]. Therefore, $CD103^+$ cells in the CT-ST and IM compartments showed less prognostic contribution compared to $CD103^+$ cells in the CT-IEL compartment, potentially due to the heterogeneous immune cell infiltration within the CT-ST and IM compartments.

There is a growing body of evidence indicating that the immune cells have a profound impact on the prognosis of tumor patients. Galon and colleagues have developed a standardized method for assessing lymphocyte immune infiltration, which entails analyzing the combined populations of $CD8^+$ and $CD3^+$ cells within both the tumor core and the invasive margin [34, 35]. This scoring system effectively categorizes patients into high- and low-risk groups, demonstrating significant discrepancies in time to recurrence, disease-free survival, and overall survival. Galon selected the T cell marker CD3 and cytotoxic T cell marker CD8 for their staining quality and antigen stability. With a deeper understanding of the tumor immune microenvironment, a potential future immune scoring system could encompass multiple immune parameters, including markers for cytotoxic T cells, memory T cells, T cell exhaustion, and immune suppression. To enhance the prognostic value of $CD103^+$ cells in CRC, we devised an CD103 score based on the presence of $CD103^+$ cells in distinct intratumor compartments. In the discovery cohort and validation cohort, the relative contribution of a single compartment of $CD103^+$ cells alone to predict survival was found to be inferior to that of vascular invasion or N stage. Nonetheless, a combined analysis of $CD103^+$ cells in intratumor compartments showed superior predictive power than that of vascular invasion and N stage. Specifically, the power of the CD103 score to forecast CSS and DFS was nearly five times greater than that of the N stage in the whole cohort. In high-risk patients with lymph node metastasis, CD103 score also allowed the identification of patients with distinct clinical outcome for CSS and DFS. Patients with an Hi CD103 score exhibited significantly improved survival compared to those in the other two groups. However, the survival curves of patients in the Int and Lo CD103 score groups overlapped, indicating that the presence of only one or two compartments with high $CD103^+$ cell infiltration may not be sufficient to accurately predict survival in this patient population. Thus, an integrated examination of $CD103^+$ cells across different intratumor compartments revealed improved predictive value for survival outcomes among diverse CRC patient groups compared to analyzing a single compartment alone. However, the potential limitation of this CD103 score may arise from its dependence on a single immune parameter. In agreement with our findings, studies have showed that a significant of $CD103^+$ cells in the tumor microenvironment concurrently express the CD8 molecule [16]. Furthermore, $CD103^+CD8^+$ cells demonstrated a more pronounced tissue-resident signature and anti-tumor efficacy in comparison to $CD103^-CD8^+$ cells [36]. The infiltration of intratumor $CD103^+$ cells presented a superior prognostic value than $CD8^+$ cells in various cancers [12, 14, 27, 37]. Hence, a combined evaluation of CD103, rather than CD8, along with other immune parameters in the CT-IEL, CT-ST, and IM compartments may serve as a valuable immune scoring system for assessing the degree of antitumor immunity.

Our study has certain limitations, including the reliance on the pathologist's clinical experience and personal discretion in selecting representative compartments for $CD103^+$ cell infiltration. This approach may introduce selectivity bias and inefficiency, posing challenges for clinical applicability. Incorporating machine learning techniques to identify and quantify $CD103^+$ cell infiltration could potentially mitigate these limitations and improve the accuracy and efficiency of the analysis. Moreover, a limited number of patients underwent testing for MSS/MSI status, which hindered a comprehensive evaluation of the impact of MSS/MSI status on the infiltration of $CD103^+$ cells. Additionally, as these patients did not receive any form of immunotherapy, the potential role of $CD103^+$ cells in intratumor compartments in predicting response to immunotherapy remained uncertain.

To conclude, our present study investigated the intratumor compartment and phenotype of $CD103^+$ cells within CRC tissues, suggesting that the infiltration of $CD103^+$ cells in various intratumor compartments could be a significant prognostic factor for CRC patients. Tumor-specific $CD103^+CD8^+$ TRM cells are crucial in the anti-tumor immune response, but further investigation is needed to elucidate their precise role in tumor biology, which appears

to be influenced by their intratumor locations and activation status. Understanding this mechanism could provide valuable insights for the development of immunotherapy strategies for colorectal cancer.

Supplementary Information The online version contains supplementary material available at https://doi.org/10.1007/s00262-025-04087-z.

Acknowledgements None.

Author's contribution Guarantor of integrity of the entire study: MH and PH. Manuscript preparation: AH, YW, MA and HY. Experiments and data analysis: AH, YW and YX. Sample collection: JC, MC and JZ. Manuscript revision: MH and PH. All authors read and approved the final manuscript.

Funding Support for these studies was provided by the Natural Science Foundation of Guangdong Province (2022A1515012457, JC), the Sixth Affiliated Hospital of Sun Yat-sen University Clinical Research-'1010' Program (1010CG(2022)-02, MH), the Fundamental Research Funds for the Central Universities, Sun Yat-sen University (2022007, MH).

Data availability The datasets used and/or analyzed during the current study are available from the corresponding author upon reasonable request. No datasets were generated or analysed during the current study.

Declarations

Conflict of interest The authors declare no competing interests.

Ethics approval and consent to participate Written informed consent was obtained from each patient, and the study was approved by the Clinical Research Ethics Committee of the Sixth Affiliated Hospital and the Cancer Center of Sun Yat-sen University.

Consent for publication All the authors agree to publish this paper.

References

1. Bray F, Laversanne M, Sung H, Ferlay J, Siegel RL, Soerjomataram I, Jemal A (2024) Global cancer statistics 2022: GLOBOCAN estimates of incidence and mortality worldwide for 36 cancers in 185 countries. CA Cancer J Clin. https://doi.org/10.3322/caac.21834
2. Dekker E, Tanis PJ, Vleugels JLA, Kasi PM, Wallace MB (2019) Colorectal cancer. Lancet 394:1467–1480. https://doi.org/10.1016/S0140-6736(19)32319-0
3. Xie Y, Shi L, He X, Luo Y (2021) Gastrointestinal cancers in China, the USA, and Europe. Gastroenterol Rep (Oxf) 9:91–104. https://doi.org/10.1093/gastro/goab010
4. Galon J, Mlecnik B, Bindea G et al (2014) Towards the introduction of the "Immunoscore" in the classification of malignant tumours. J Pathol 232:199–209. https://doi.org/10.1002/path.4287
5. Mlecnik B, Tosolini M, Kirilovsky A et al (2011) Histopathologic-based prognostic factors of colorectal cancers are associated with the state of the local immune reaction. J Clin Oncol 29:610–618. https://doi.org/10.1200/JCO.2010.30.5425
6. Fridman WH, Pages F, Sautes-Fridman C, Galon J (2012) The immune contexture in human tumours: impact on clinical outcome. Nat Rev Cancer 12:298–306. https://doi.org/10.1038/nrc3245
7. Whiteside TL, Demaria S, Rodriguez-Ruiz ME, Zarour HM, Melero I (2016) Emerging Opportunities and challenges in cancer immunotherapy. Clin Cancer Res 22:1845–1855. https://doi.org/10.1158/1078-0432.CCR-16-0049
8. Bai Z, Zhou Y, Ye Z, Xiong J, Lan H, Wang F (2021) Tumor-infiltrating lymphocytes in colorectal cancer: the fundamental indication and application on immunotherapy. Front Immunol 12:808964. https://doi.org/10.3389/fimmu.2021.808964
9. Byrne A, Savas P, Sant S et al (2020) Tissue-resident memory T cells in breast cancer control and immunotherapy responses. Nat Rev Clin Oncol 17:341–348. https://doi.org/10.1038/s41571-020-0333-y
10. Mami-Chouaib F, Blanc C, Corgnac S, Hans S, Malenica I, Granier C, Tihy I, Tartour E (2018) Resident memory T cells, critical components in tumor immunology. J Immunother Cancer 6:87. https://doi.org/10.1186/s40425-018-0399-6
11. Duhen T, Duhen R, Montler R et al (2018) Co-expression of CD39 and CD103 identifies tumor-reactive CD8 T cells in human solid tumors. Nat Commun 9:2724. https://doi.org/10.1038/s41467-018-05072-0
12. Webb JR, Milne K, Watson P, Deleeuw RJ, Nelson BH (2014) Tumor-infiltrating lymphocytes expressing the tissue resident memory marker CD103 are associated with increased survival in high-grade serous ovarian cancer. Clin Cancer Res 20:434–444. https://doi.org/10.1158/1078-0432.CCR-13-1877
13. Wang ZQ, Milne K, Derocher H, Webb JR, Nelson BH, Watson PH (2016) CD103 and intratumoral immune response in breast cancer. Clin Cancer Res 22:6290–6297. https://doi.org/10.1158/1078-0432.CCR-16-0732
14. Djenidi F, Adam J, Goubar A, Durgeau A, Meurice G, de Montpreville V, Validire P, Besse B, Mami-Chouaib F (2015) CD8+CD103+ tumor-infiltrating lymphocytes are tumor-specific tissue-resident memory T cells and a prognostic factor for survival in lung cancer patients. J Immunol 194:3475–3486. https://doi.org/10.4049/jimmunol.1402711
15. Hu X, Li YQ, Li QG, Ma YL, Peng JJ, Cai SJ (2018) ITGAE defines CD8+ tumor-infiltrating lymphocytes predicting a better prognostic survival in colorectal cancer. EBioMedicine 35:178–188. https://doi.org/10.1016/j.ebiom.2018.08.003
16. Nizard M, Roussel H, Diniz MO et al (2017) Induction of resident memory T cells enhances the efficacy of cancer vaccine. Nat Commun 8:15221. https://doi.org/10.1038/ncomms15221
17. Allakhverdi Z, Fitzpatrick D, Boisvert A, Baba N, Bouguermouh S, Sarfati M, Delespesse G (2006) Expression of CD103 identifies human regulatory T-cell subsets. J Allergy Clin Immunol 118:1342–1349. https://doi.org/10.1016/j.jaci.2006.07.034
18. Anz D, Mueller W, Golic M et al (2011) CD103 is a hallmark of tumor-infiltrating regulatory T cells. Int J Cancer 129:2417–2426. https://doi.org/10.1002/ijc.25902

19. Lin YC, Chang LY, Huang CT, Peng HM, Dutta A, Chen TC, Yeh CT, Lin CY (2009) Effector/memory but not naive regulatory T cells are responsible for the loss of concomitant tumor immunity. J Immunol 182:6095–6104. https://doi.org/10.4049/jimmunol.0803829
20. Fu C, Jiang A (2018) Dendritic cells and CD8 T cell immunity in tumor microenvironment. Front Immunol 9:3059. https://doi.org/10.3389/fimmu.2018.03059
21. Steele KE, Tan TH, Korn R et al (2018) Measuring multiple parameters of CD8+ tumor-infiltrating lymphocytes in human cancers by image analysis. J Immunother Cancer 6:20. https://doi.org/10.1186/s40425-018-0326-x
22. Yang G, Cai S, Hu M et al (2023) Functional status and spatial architecture of tumor-infiltrating CD8+ T cells are associated with lymph node metastases in non-small cell lung cancer. J Transl Med 21:320. https://doi.org/10.1186/s12967-023-04154-y
23. Vayrynen JP, Kantola T, Vayrynen SA et al (2016) The relationships between serum cytokine levels and tumor infiltrating immune cells and their clinical significance in colorectal cancer. Int J Cancer 139:112–121. https://doi.org/10.1002/ijc.30040
24. Sinicrope FA, Rego RL, Ansell SM, Knutson KL, Foster NR, Sargent DJ (2009) Intraepithelial effector (CD3+)/regulatory (FoxP3+) T-cell ratio predicts a clinical outcome of human colon carcinoma. Gastroenterology 137:1270–1279. https://doi.org/10.1053/j.gastro.2009.06.053
25. Lee WS, Park S, Lee WY, Yun SH, Chun HK (2010) Clinical impact of tumor-infiltrating lymphocytes for survival in stage II colon cancer. Cancer 116:5188–5199. https://doi.org/10.1002/cncr.25293
26. Gu Y, Chen Y, Jin K et al (2020) Intratumoral CD103(+)CD4(+) T cell infiltration defines immunoevasive contexture and poor clinical outcomes in gastric cancer patients. Oncoimmunology 9:1844402. https://doi.org/10.1080/2162402X.2020.1844402
27. Wang B, Wu S, Zeng H et al (2015) CD103+ tumor infiltrating lymphocytes predict a favorable prognosis in urothelial cell carcinoma of the bladder. J Urol 194:556–562. https://doi.org/10.1016/j.juro.2015.02.2941
28. Zhou Q, Ou Y, Dai X et al (2023) Prevalence of tumour-infiltrating CD103(+) cells identifies therapeutic-sensitive prostate cancer with poor clinical outcome. Br J Cancer 128:1466–1477. https://doi.org/10.1038/s41416-023-02183-4
29. Overgaard NH, Jung JW, Steptoe RJ, Wells JW (2015) CD4+/CD8+ double-positive T cells: more than just a developmental stage? J Leukoc Biol 97:31–38. https://doi.org/10.1189/jlb.1RU0814-382
30. Parrot T, Oger R, Allard M et al (2020) Transcriptomic features of tumour-infiltrating CD4(low)CD8(high) double positive alphabeta T cells in melanoma. Sci Rep 10:5900. https://doi.org/10.1038/s41598-020-62664-x
31. Menard LC, Fischer P, Kakrecha B et al (2018) Renal cell carcinoma (RCC) tumors display large expansion of double positive (DP) CD4+CD8+ T cells with expression of exhaustion markers. Front Immunol 9:2728. https://doi.org/10.3389/fimmu.2018.02728
32. Sarrabayrouse G, Corvaisier M, Ouisse LH, Bossard C, Le Mevel B, Potiron L, Meurette G, Gervois N, Jotereau F (2011) Tumor-reactive CD4+ CD8alphabeta+ CD103+ alphabetaT cells: a prevalent tumor-reactive T-cell subset in metastatic colorectal cancers. Int J Cancer 128:2923–2932. https://doi.org/10.1002/ijc.25640
33. Godefroy E, Alameddine J, Montassier E et al (2018) Expression of CCR6 and CXCR6 by gut-derived CD4(+)/CD8alpha(+) T-regulatory cells, which are decreased in blood samples from patients with inflammatory bowel diseases. Gastroenterology 155:1205–1217. https://doi.org/10.1053/j.gastro.2018.06.078
34. Pages F, Mlecnik B, Marliot F et al (2018) International validation of the consensus Immunoscore for the classification of colon cancer: a prognostic and accuracy study. Lancet 391:2128–2139. https://doi.org/10.1016/S0140-6736(18)30789-X
35. Mlecnik B, Bifulco C, Bindea G et al (2020) Multicenter international society for immunotherapy of cancer study of the consensus immunoscore for the prediction of survival and response to chemotherapy in stage III colon cancer. J Clin Oncol 38:3638–3651. https://doi.org/10.1200/JCO.19.03205
36. Ganesan AP, Clarke J, Wood O et al (2017) Tissue-resident memory features are linked to the magnitude of cytotoxic T cell responses in human lung cancer. Nat Immunol 18:940–950. https://doi.org/10.1038/ni.3775
37. Komdeur FL, Prins TM, van de Wall S et al (2017) CD103+ tumor-infiltrating lymphocytes are tumor-reactive intraepithelial CD8+ T cells associated with prognostic benefit and therapy response in cervical cancer. Oncoimmunology 6:e1338230. https://doi.org/10.1080/2162402X.2017.1338230